




Article

Sparse Adaptive Iteratively-Weighted Thresholding Algorithm (SAITA) for L_p -Regularization Using the Multiple Sub-Dictionary Representation

Yunyi Li ¹ , Jie Zhang ², Shangang Fan ², Jie Yang ² , Jian Xiong ², Xiefeng Cheng ¹, Hikmet Sari ², Fumiyuki Adachi ³ and Guan Gui ^{2,*} 

¹ College of Electronic and Optical Engineering & College of Microelectronics, Nanjing University of Posts and Telecommunications, Nanjing 210023, China; 2016020221@njupt.edu.cn (Y.L.); chengxf@njupt.edu.cn (X.C.)

² College of Telecommunication and Information Engineering, Nanjing University of Posts and Telecommunications, Nanjing 210023, China; b13011409@njupt.edu.cn (J.Z.); sponder@126.com (S.F.); jyang@njupt.edu.cn (J.Y.); jxiong@njupt.edu.cn (J.X.); hikmet@njupt.edu.cn (H.S.)

³ Research Organization of Electrical Communication, Tohoku University, Sendai 980-8577, Japan; adachi@ecei.tohoku.ac.jp

* Correspondence: guiguan@njupt.edu.cn

Received: 19 October 2017; Accepted: 13 December 2017; Published: 15 December 2017

Abstract: Both $L_{1/2}$ and $L_{2/3}$ are two typical non-convex regularizations of L_p ($0 < p < 1$), which can be employed to obtain a sparser solution than the L_1 regularization. Recently, the multiple-state sparse transformation strategy has been developed to exploit the sparsity in L_1 regularization for sparse signal recovery, which combines the iterative reweighted algorithms. To further exploit the sparse structure of signal and image, this paper adopts multiple dictionary sparse transform strategies for the two typical cases $p \in \{1/2, 2/3\}$ based on an iterative L_p thresholding algorithm and then proposes a sparse adaptive iterative-weighted L_p thresholding algorithm (SAITA). Moreover, a simple yet effective regularization parameter is proposed to weight each sub-dictionary-based L_p regularizer. Simulation results have shown that the proposed SAITA not only performs better than the corresponding L_1 algorithms but can also obtain a better recovery performance and achieve faster convergence than the conventional single-dictionary sparse transform-based L_p case. Moreover, we conduct some applications about sparse image recovery and obtain good results by comparison with relative work.

Keywords: L_p -norm regularization; adaptive weighted; iterative thresholding; multiple dictionaries; single-dictionary; image restoration

1. Introduction

Compressed sensing (CS) [1,2] and sparse representation [3,4] have been widely used in the field of wireless communications [5–7] and image processing [8–10]. CS implies that it is possible to reconstruct the sparse signal/image from incomplete data if some prior knowledge and reconstruction constraints are satisfied. Mathematically, the unconstrained L_0 minimization is the optimal model to obtain the sparsest solution $\hat{\mathbf{x}}_{l_0}$:

$$\hat{\mathbf{x}}_{l_0} = \arg \min_{\mathbf{x}} \{ \gamma \| \mathbf{y} - \Phi \mathbf{x} \|_2^2 + \lambda \| \mathbf{x} \|_0 \}, \quad (1)$$

where $\| \mathbf{x} \|_0$ denotes the zero-norm function to find the number of nonzero elements in \mathbf{x} ; $\Phi \in R^{M \times N}$ denotes the down-sampling measurement matrix; \mathbf{y} and \mathbf{x} represent the observed vector and the unknown sparse image, respectively; λ is the regularization parameter to balance between the fidelity

of the image and the sparsity; and $\gamma > 0$ is a small positive constant, e.g., $\gamma = 1/2$. Unfortunately, this problem (1) is an NP (non-deterministic) problem, and thus, it is difficult to efficiently solve. When the matrix Φ satisfies some necessary conditions [11], an alternative convex relaxation method are developed using the L_1 regularization method as:

$$\hat{\mathbf{x}}_{l_p} = \arg \min_{\hat{\mathbf{x}}} \{ \gamma \| \mathbf{y} - \Phi \mathbf{x} \|_2^2 + \lambda \| \mathbf{x} \|_1 \}, \quad (2)$$

where $\| \mathbf{x} \|_1 = \sum_{i=1}^n |x_i|$ denotes the L_1 -norm. Then, the NP problem (1) is converted into problem (2), which is a typical a convex optimization problem and can be solved efficiently, such as with the alternating direction method of multipliers (ADMM) [12,13], fast iterative shrinkage-thresholding algorithm (FISTA) [14], Nesterov's algorithm (NESTA) [15], and approximate message passing (AMP) [16]. However, the method of L_1 regularization can only obtain a suboptimal solution and usually requires much more measurements. Theoretical analysis of CS implies that better performance can be obtained by taking advantage of sparser information in many systems, especially in the presence of strong noise interference.

1.1. The Non-Convex Penalties

Many state-of-the-art algorithms have been proposed to improve the performance of the L_1 regularization algorithms. The non-convex penalty regularization algorithms are among the most effective algorithms for sparse recovery problems. Research shows that the non-convex penalty-based optimization methods can more closely approximate the sparsest solution over the L_1 -norm penalty in problem (2), which requires a weaker incoherent condition and fewer measurement data [17]. There have been many non-convex functions proposed as relaxations of the L_0 -norm penalty, such as the smoothly clipped absolute deviation penalty (SCAD) [18], the L_p , ($0 < p < 1$)-norm penalty [17] and the minimax concave penalty (MCP) [19]. By replacing the L_1 -norm with the L_p -norm, the non-convex L_p -norm regularization optimization method is described as:

$$\hat{\mathbf{x}}_{l_p} = \arg \min_{\hat{\mathbf{x}}} \{ \gamma \| \mathbf{y} - \Phi \mathbf{x} \|_2^2 + \lambda \| \mathbf{x} \|_p^p \}, \quad 0 < p < 1, \quad (3)$$

where $\| \mathbf{x} \|_p^p = \sum_{i=1}^n |x_i|^p$. Unfortunately, when $0 < p < 1$, problem (3) becomes a non-convex, non-smooth, and non-Lipschitz optimization problem. Thus, the L_p -norm optimization is always difficult to efficiently address.

1.2. The Iterative Thresholding Algorithm of L_p Regularization

There are two main classes of algorithms to solve the non-convex L_p -norm optimization problem. One is the iteratively reweighted algorithm [20], and the other is the iterative thresholding algorithm (ITA). As one of the most effective and efficient methods, the ITA has been employed for many sparse recovery optimization problems due to its low computational complexities, including the iterative hard thresholding for L_0 regularization [21], the iterative soft thresholding for L_1 regularization [22] and the iterative L_p thresholding for L_p regularization [23]. $L_{1/2}$ and $L_{2/3}$ regularizations are two special and important cases, not only their solutions can be expressed in closed-forms, but also their importance on sparse modeling. Recent studies show that $L_{1/2}$ regularizer can be taken as the most representative L_p regularizer [24] and $L_{2/3}$ regularization is more effective in image deconvolution problem [25]. Hence, in this paper, we focus on the $L_{1/2}$ and $L_{2/3}$ regularizations, which is described in Equation (4) and (5):

$$\hat{\mathbf{x}}_{l_{1/2}} = \arg \min_{\hat{\mathbf{x}}} \{ \gamma \| \mathbf{y} - \Phi \mathbf{x} \|_2^2 + \lambda \| \mathbf{x} \|_{1/2}^{1/2} \}, \quad (4)$$

$$\hat{\mathbf{x}}_{l_{2/3}} = \arg \min_{\hat{\mathbf{x}}} \{ \gamma \| \mathbf{y} - \Phi \mathbf{x} \|_2^2 + \lambda \| \mathbf{x} \|_{2/3}^{2/3} \}, \quad (5)$$

1.3. New Multiple-State Sparse Transform Based L_1 Regularization Algorithm

Recently, some new multiple-state sparse transform based algorithms were proposed to exploit more a priori knowledge of the signal/image by employing some new sparsifying transform strategies. A shearlet-based multiple level sparse representation algorithmic framework was proposed in [26,27] for the unconstrained L_1 regularization by adaptively incorporating the iteratively reweighted shrinkage step. To enhance the sparsity, the algorithm [27] is specifically adapted to the sparse structure of the multiscale coefficients based on the ADMM [12,13]. Similarly, considering the fact that the sparsity of a certain signal/image will change under different sparsifying transform dictionaries, a sparsity-induced composite regularization algorithm was proposed for the unconstrained L_1 regularization problem (Co-L1) [28]. The novel Co-L1 method is described as:

$$\hat{\mathbf{x}}_{d,1}^t = \arg \min_{\hat{\mathbf{x}}} \left\{ \|\Phi \mathbf{x} - \mathbf{y}\|_2^2 + \sum_{d=1}^D \lambda_{d,1} \|\Psi_d \mathbf{x}\|_1 \right\}, \quad (6)$$

where $\Psi_d = [\psi_1 | \psi_2 | \dots | \psi_{N_d}] \in R^{N_d \times N}$, ($d = 1, \dots, D$) are different dictionaries, d denotes the number of Ψ_d , and N_d represents the dictionary size. The regularization parameters $\lambda_{d,1} = \frac{N_d}{\varepsilon + \|\Psi_d \mathbf{x}\|_1}$ play the roles of weighting the L_1 -norm of the sparsifying transform coefficients $\Psi_d \mathbf{x}$. Multiplying by the weighting parameter $\lambda_{d,1}^t = \left[\frac{N_1}{\varepsilon + \|\Psi_1 \mathbf{x}\|_1}, \dots, \frac{N_d}{\varepsilon + \|\Psi_d \mathbf{x}\|_1} \right]^T$, the regularizer $\sum_{d=1}^D \lambda_{d,1} \|\Psi_d \mathbf{x}\|_1$ is indeed a composition of multiple dictionary based regularizers. The algorithm [28] can significantly improve the image reconstruction performance over the fast iterative shrinkage-thresholding algorithm (FISTA) [29] by iteratively and adaptively weighting the composite regularizer. We define these new emerged sparsifying transforms as the “multiple-state” transform. The common property of these methods is how to exploit the prior information from the multiple-state sparsifying transform to improve the conditioning of the sparse recovery problems.

In this paper, benefiting from the improvement of the L_p regularization algorithm [24,25,30], and motivated by recent advances in the iterative reweighted algorithms, we propose a new iteratively-weighted algorithm framework for L_p , $p \in \{1/2, 2/3\}$, norm minimization using the multiple-state sparsifying transform, i.e., multiple sub-dictionary sparse representation [28]. The contributions of this paper are summarized as follows. (1) Based on the multiple sub-dictionary sparse representation, we develop a new iteratively-weighted L_p ($p \in \{1/2, 2/3\}$) thresholding algorithm, which is called as SAITA- L_p ($p \in \{1/2, 2/3\}$). (2) By comparison with the existing iteratively-reweighted parameter scheme, we propose an updating regularization parameter for weighting the sub-dictionary. (3) $L_{1/2}$ regularization and $L_{2/3}$ regularization are special and important on sparse modeling, particularly on sparse recovery. However, related studies are rare, this paper also extend the applications to sparse image recovery and Magnetic resonance imaging (MRI) and get good results.

The organization of the rest of the paper is as follows: in Section 2, we propose the multiple sub-dictionary L_p -regularization in the SAITA- L_p algorithm, including the multiple sub-dictionary sparsifying transforms and the iterative reweighted scheme for the SAITA- L_p regularizer. Then, in Section 3, we develop a new L_p norm minimization, iteratively thresholding algorithm SAITA- L_p . To confirm the proposed algorithm, we conduct simulations and applications in image restorations in Section 4. In Section 5, we further validate our proposed algorithm using three applications. Finally, conclusions are given in Section 6.

2. The Proposed Multiple Sub-Dictionary-Based L_p Regularization

The multiple dictionary sparsifying transform method for the L_1 regularization optimization problem was proposed in [28], which extends the well-known Lasso problem into a composite regularization problem. Motivated by the composite regularization method for the L_1 -norm, this paper employs the multiple sub-dictionary method for the L_p regularization problem.

Suppose $\mathbf{x} \in \mathbb{R}^{N \times 1}$ is the non-sparse, raw signal. We can obtain the sparse coefficients $\Psi \mathbf{x}$ through an analysis dictionary $\Psi \in \mathbb{R}^{N_1 \times N}$. The shearlet transform [31] and the wavelet transform [32] are two typical sparsifying transforms. We choose the wavelet transform as the ideal transform because of its effectiveness to compress natural images. The main steps to design the multiple sub-dictionary sparsifying transform based L_p regularization method are:

First, we construct an $(DN) \times N$ over-complete sparsifying transform matrix Ψ by:

$$\Psi = \begin{bmatrix} \Psi_1 \\ \vdots \\ \Psi_d \\ \vdots \\ \Psi_D \end{bmatrix} \in \mathbb{R}^{(DN) \times N}, \tag{7}$$

and:

$$\Psi_d = \begin{bmatrix} \psi_1 \\ \psi_2 \\ \vdots \\ \psi_{N_d} \end{bmatrix} \in \mathbb{R}^{N_d \times N}, \tag{8}$$

where D denotes the number of sub-dictionaries Ψ_d in the over-complete sparsifying transform matrix Ψ , the $N_d \times N$ sub-dictionary matrix Ψ_d , ($d = 1, \dots, D$) is acquired by a collection of row vectors $\{\psi_i\}_{i=1}^{N_d}$, such as the “*dbN*” wavelet basis [33], and N_d represents the number of column in ψ_i . From Equation (8) we can see that each Ψ_d is composed of a set of rows from the $(DN) \times N$ over-complete sparsifying transform matrix Ψ , and:

$$N_1 + N_2 + \dots + N_d = DN, \tag{9}$$

By splitting the matrix Ψ into several sub-dictionaries Ψ_d , we convert the sparsifying transform $\Psi \mathbf{x}$ to a composition of several $\Psi_d \mathbf{x}$, $d = 1, 2, \dots, D$ with different sparse structures. Intuitively, we can utilize these differences to improve the recovery performance in sparse recovery problems. In this paper, we choose $N_1 = N_2 = \dots = N_d = N$, so $\Psi_d \in \mathbb{R}^{N \times N}$, which are orthogonal matrixes.

Then, a new multiple non-convex L_p regularization method is proposed:

$$\hat{\mathbf{x}}_{i,d,p}^t = \arg \min_{\hat{\mathbf{x}}} \left\{ f_d(\mathbf{x}) = \gamma \| \Phi \mathbf{x} - \mathbf{y} \|_2^2 + R_{SAITA} \right\}, \tag{10}$$

where R_{SAITA} is a linearly weighted combination of multiple sub-dictionary based L_p regularizers $\| \Psi_d \mathbf{x} \|_p^p$:

$$R_{SAITA} = \sum_{d=1}^D \lambda_{d,p}^t \| \Psi_d \mathbf{x} \|_p^p = \lambda_{1,p}^t \| \Psi_1 \mathbf{x} \|_p^p + \lambda_{2,p}^t \| \Psi_2 \mathbf{x} \|_p^p + \dots + \lambda_{D,p}^t \| \Psi_D \mathbf{x} \|_p^p, \tag{11}$$

the $\lambda_{d,p}$, $d = 1, 2, \dots, D$ denotes the iterative weighted regularization parameter. Hence, the contribution of each sub-dictionary is controlled adaptively and iteratively with the weighted parameter $\lambda_{d,p}$, and the regularizer $\| \Psi_d \mathbf{x} \|_p^p$ will vary across the sub-dictionary index d . Intuitively, the variation of each sub-dictionary based regularizer is best weighted by the parameter $\lambda_{d,p}$ to improve the sparse recovery problem.

3. The Proposed SAITA- L_p Algorithm

The major disadvantage of the L_p ($0 < p < 1$) minimization is that it is nonconvex, making it difficult to efficiently solve. In this section, we first introduce the iteratively thresholding

representation theory for the conventional L_p , ($p \in \{1/2, 2/3\}$) algorithm according to the existing series of algorithms in [25,34]. Then, we deduce the SAITA- L_p algorithm combined with the proposed weighted scheme $\lambda_{d,p}$.

3.1. The Relationship of the SAITA- L_p and Conventional L_p Methods

Considering the multiple sub-dictionary L_p , ($p \in \{1/2, 2/3\}$) regularization problem in Equation (10), when $\gamma = 1$, we have:

$$\hat{\mathbf{x}}_{l_{d,p}} = \arg \min_{\hat{\mathbf{x}}} \left\{ f_d(\mathbf{x}) = \|\Phi \mathbf{x} - \mathbf{y}\|_2^2 + \sum_{d=1}^D \lambda_{d,p} \|\Psi_d \mathbf{x}\|_p^p \right\}, \quad (12)$$

where the $f_d(\mathbf{x})$ denotes the objective functions. Correspondingly, the conventional single dictionary $\Psi' \in R^{N \times N}$ based analysis L_p -norm minimization problem is as follows:

$$\hat{\mathbf{x}}_{l_p}^t = \arg \min_{\hat{\mathbf{x}}} \left\{ f(\mathbf{x}) = \|\Phi \mathbf{x} - \mathbf{y}\|_2^2 + \lambda_p \|\Psi' \mathbf{x}\|_p^p \right\}, \quad (13)$$

The proposed SAITA- L_p ($p \in \{1/2, 2/3\}$) methods of (12) and the conventional method (13) are nearly identical, and the major difference is how to weight the contribution of the L_p -norm by the regularization parameter [28]. Compared with the conventional method, the SAITA method can exploit more prior knowledge of the sparse signal/image for reconstruction. Figure 1 depicts the relationship between the two methods. In the case of (A), the number of sub-dictionaries d is reduced to 1, and the multiple dictionaries Ψ_d convert into a single Ψ . Then, the proposed SAITA- L_p algorithm converts to the conventional single dictionary L_p method [24,25]. In case (B), with the increase of the number d , the conventional single dictionary L_p method converts to the proposed SAITA- L_p method.

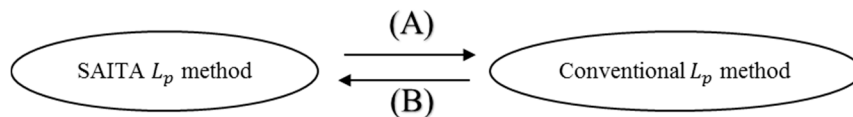


Figure 1. The relationship between the conventional single dictionary based L_p thresholding method and the proposed SAITA L_p method.

3.2. The Thresholding Representation Theory for SAITA- L_p

According to the relationship between the proposed SAITA- L_p method and the conventional L_p method shown in Figure 1, we first consider the conventional single dictionary analysis L_p problem (13). The first order optimality condition of \mathbf{x} is described as:

$$\nabla f(\mathbf{x}) = 2\Psi' \Phi^T (\Phi \mathbf{x} - \mathbf{y}) + \lambda \nabla (\|\Psi' \mathbf{x}\|_p^p) \quad (14)$$

in which the operator $\nabla(\cdot)$ denotes the gradient. Letting $\nabla f(\mathbf{x}) = 0$, we have:

$$\Psi' \Phi^T (\mathbf{y} - \Phi \mathbf{x}) = \frac{1}{2} (\lambda \nabla (\|\Psi' \mathbf{x}\|_p^p)), \quad (15)$$

Multiplying by any parameter τ to control the step size and adding $\Psi' \mathbf{x}$ in both sides of Equation (15):

$$\Psi' \mathbf{x} + \tau \Psi' \Phi^T (\mathbf{y} - \Phi \mathbf{x}) = \Psi' \mathbf{x} + \frac{1}{2} (\lambda \tau \nabla (\|\Psi' \mathbf{x}\|_p^p)), \quad (16)$$

Then, we can immediately obtain:

$$\left(\mathbf{I} + \frac{\lambda \tau}{2} \nabla (\|\cdot\|_p^p) \right) \Psi' \mathbf{x} = \Psi' \mathbf{x} + \tau \Psi' \Phi^T (\mathbf{y} - \Phi \mathbf{x}) \quad (17)$$

That is:

$$\Psi' \mathbf{x} = \left(\mathbf{I} + \frac{\lambda \tau}{2} \nabla(\|\cdot\|_p^p) \right)^{-1} \Psi' (\mathbf{x} + \tau \Phi^T (\mathbf{y} - \Phi \mathbf{x})) \quad (18)$$

To this end, when $p \in \{1/2, 2/3\}$, the resolvent operator [24,25,30] is denoted as:

$$H_{\lambda,p}(\cdot) = \left(\mathbf{I} + \frac{\lambda \tau}{2} \nabla(\|\cdot\|_p^p) \right)^{-1}, \quad (19)$$

where λ and τ are the regularization parameter and the step tuning parameter, respectively. Then:

$$\Psi' \mathbf{x} = H_{\lambda,p} \left(\Psi' (\mathbf{x} + \tau \Phi^T (\mathbf{y} - \Phi \mathbf{x}^n)) \right), \quad (20)$$

where $\tau > 0$ (e.g., $\tau = \frac{0.99}{\|\Phi\|_2^2}$, or $\tau = \frac{0.99}{\|\Phi\|_2}$) controls the step size in each iteration.

According to the Equation (20), we immediately imply:

$$\mathbf{x}^{n+1} = (\Psi')^{-1} H_{\lambda,p}(\theta(\mathbf{x}^n)), \quad (21)$$

in which:

$$\theta(\mathbf{x}^n) = \Psi' (\mathbf{x}^n + \tau \Phi^T (\mathbf{y} - \Phi \mathbf{x}^n)), \quad (22)$$

where \mathbf{x}^n represents the n -th iterative solution. The resolvent operator $H_{\lambda,p}(\cdot)$ is defined as:

$$H_{\lambda,p}(x) = (h_{\lambda,p}(x_1), h_{\lambda,p}(x_2), \dots, h_{\lambda,p}(x_N))^T, \quad (23)$$

where the $h_{\lambda,p}(x_i)$ is the nonlinear function defined by:

$$h_{\lambda,p}(x_i) = \begin{cases} \varphi_{\lambda,p}(x_i), & |x_i| > T \\ 0, & \text{otherwise} \end{cases}, \quad (24)$$

when $p = \frac{1}{2}$; $T = \frac{3\sqrt[3]{2}}{4} (\lambda_{d,1/2} \tau)^{2/3}$ is the threshold value, and [24]:

$$\varphi_{\lambda,1/2}(x_i) = \frac{2}{3} x_i \left(1 + \cos \left(\frac{2\pi}{3} - \frac{2}{3} \cos^{-1} \left(\frac{\lambda_{d,1/2} \tau}{8} \left(\frac{|x_i|}{3} \right)^{-\frac{3}{2}} \right) \right) \right), \quad (25)$$

when $p = \frac{2}{3}$; $T = \frac{2\sqrt[4]{3}}{3} (\lambda_{d,2/3} \tau)^{3/4}$ is the related threshold value, and [25]:

$$\varphi_{\lambda,2/3}(x_i) = \left(\frac{\vartheta_{\lambda,2/3}(x_i) + \sqrt{\frac{2|x|}{|\vartheta_{\lambda,2/3}(x_i)|} - |\vartheta_{\lambda,2/3}(x_i)|^2}}{2} \right)^3 \cdot \text{sgn}(t), \quad (26)$$

where $\text{sgn}(\cdot)$ denotes the sign function and

$$\vartheta_{\lambda,2/3}(x_i) = \frac{2}{\sqrt{3}} (\lambda_{d,2/3} \tau)^{1/4} \left(\cosh \left(\frac{1}{3} \text{arccosh} \left(\frac{27}{16} (\lambda_{d,2/3} \tau)^{-3/2} x_i^2 \right) \right) \right)^{1/2} \quad (27)$$

3.3. The Proposed SAITA- L_p Algorithm

As mentioned above, the iteratively weighted parameter plays a key role during the optimization process for the sparse recovery problem. For the proposed SAITA- L_p method, the iteratively weighted parameter $\lambda_{d,p}$ mainly plays two roles. One is the role of controlling the tradeoff of the fidelity and the prior knowledge between the quadratic term and the regularizer, and the other role is controlling the contribution of each regularizer. Unfortunately, it is not clear how to do this because setting an ideal

parameter is not straightforward. In [28], an iteratively updating parameter was reduced by applying a Maximization-Minimization algorithm shown as:

$$\lambda_{d,1} = \frac{N_d}{\epsilon + \|\Psi_d \mathbf{x}\|_1^1} \quad (28)$$

where N_d controls the sub-dictionary size, $\epsilon > 0$ is a small constant which prevents the denominator from zero. From Equation (28) we can obtain some useful information about setting a proper regularization parameter. Firstly, the contribution of the denominator in Equation (28) is to counterweigh each sub-dictionary based regularizer; Secondly, the numerator N_d controls the size of each sub-dictionary. Inspired by the above insights, in this paper, we design the important iteratively weighted parameter $\lambda_{d,p}$ as:

$$\lambda_{d,p} = \frac{N_d}{(\epsilon + \|\Psi_d \mathbf{x}\|_2^2)^\alpha}, \quad (29)$$

where N_d controls the sub-dictionary size as shown in [28], $\alpha \in (0, 2)$ is a small constant to tune it that is determined from the following experimental results. Then the parameter $\lambda_{d,p}^t$ plays the role of weighting each L_p -norm regularizer adaptively.

The following are the analytical justifications. (i) When signal \mathbf{x} is sparser under any dictionary of Ψ_d than others, the value of each regularizer $\|\Psi_d \mathbf{x}\|_p^p$ is smaller. Hence, the dictionary of Ψ_d is more appropriate, and on the other hand, a smaller regularizer $\|\Psi_d \mathbf{x}\|_p^p$ will be beneficial to minimizing the objective function. Thus, the weight of the regularizer should be enhanced. (ii) When the signal \mathbf{x} may not be sparse enough under another dictionary Ψ_d , that is, the dictionary of Ψ_d is not ideal, the value of $\|\Psi_d \mathbf{x}\|_p^p$ will be larger. The larger $\|\Psi_d \mathbf{x}\|_p^p$ will not be helpful to minimizing the objective function; thus the weight of the $\|\Psi_d \mathbf{x}\|_p^p$ should be smaller to counterweigh the regularizer.

For the main comparison, the conventional single-dictionary based L_p , $p \in \{1/2, 2/3\}$ -regularization method in problem (13) will be considered, and the tradeoff parameter λ_p is a fixed constant, which is shown as:

$$\lambda_p = \frac{1}{(\epsilon + \|\Psi \mathbf{x}\|_2^2)^\alpha}. \quad (30)$$

From Equation (30), we find that the conventional single-dictionary based parameter λ_p is a constant and will not vary.

Moreover, we employ the forward-backward linear strategy to accelerate the convergence of the proposed algorithm as [14]:

$$\mu^{n+1} = \frac{1 + \sqrt{1 + 4(\mu^n)^2}}{2}, \quad (31)$$

and:

$$\mathbf{x}^{n+1} = \mathbf{x}^n + \frac{\mu^n - 1}{\mu^{n+1}} (\mathbf{x}^n - \mathbf{x}^{n-1}), \quad (32)$$

The proposed iteratively-weighted SAITA- L_p algorithm can be described in Algorithm 1.

Algorithm 1: The proposed SAITA- L_p algorithm.

Problem: $\mathbf{x}^{n+1} = \operatorname{argmin}_{\mathbf{x}} \gamma \|\Phi \mathbf{x} - \mathbf{y}\|_2^2 + \sum_{d=1}^D \lambda_{d,p} \|\Psi_d \mathbf{x}\|_p^p$;

1: Input: $\{\Psi_d\}_{d=1}^D, \mathbf{y}, \Phi; L_d; \gamma = 1; \varepsilon > 0$;

2: Initialization: $n = 0; \varepsilon = 0.01; \tau = \frac{1-\varepsilon}{\|\Phi\|^2}; \lambda_{d,1/2}^{(1)} = 1; \alpha$.

3: for $n = 1, 2, 3, \dots$

4: Calling the conventional analysis L_p algorithm in (13):

While not converged do

Step 1: Compute $\theta(\mathbf{x}^n) = \Psi'(\mathbf{x}^n + \Phi^T(\mathbf{y} - \Phi \mathbf{x}^n))$ in Equation (22);

Step 2: Compute $\mathbf{x}^{n+1} = (\Psi')^{-1} H_{\lambda,p}(\theta(\mathbf{x}^n))$ in Equation (21);

Step 3: Update the value of μ using $\mu^{n+1} = \frac{1 + \sqrt{1 + 4(\mu^n)^2}}{2}$ in Equation (31);

Step 4: Update the solution $\mathbf{x}^{n+1} = \mathbf{x}^n + \frac{\mu^n - 1}{\mu^{n+1}}(\mathbf{x}^n - \mathbf{x}^{n-1})$ in Equation (32);

End

5: Updating: $\lambda_{d,p}^{(n+1)} \leftarrow \frac{N_d}{(\varepsilon + \|\Psi_d \mathbf{x}^{(n)}\|_2^2)^\alpha}$ in Equation (29);

6: end

7: Output \mathbf{x}^t

4. Performance Analysis and Discussion

We first conduct some experiments to determine the value of α and verify the performance of the proposed $\lambda_{d,p}^t$, then we evaluate the superiority of the proposed SAITA algorithm compared with the conventional single dictionary analysis L_p iterative thresholding algorithms [24,25] and the Co-L1 [28]. All the experiments in this paper were conducted on a personal computer (2.21 GHz, 16 GB RAM) in a MATLAB (R2014a) platform.

Assuming the clean image \mathbf{x} , we construct a measurement matrix Φ using the ‘‘Spread Spectrum’’ operator [35], so the measurement image shows: $\mathbf{y} = \Phi \mathbf{x} + \mathbf{n}$, where \mathbf{n} denotes the additive noise. Since the wavelet is known to compress natural raw images very efficiently, we choose the wavelet transform as the sparsifying transform operator. Then, we construct the sparsifying transform matrix $\Psi \in \mathbb{R}^{8N \times N}$ by concatenating the undecimated ‘db1’ and ‘db2’ wavelet transform with 2-levels of decomposition. Thus, we can obtain the sub-dictionaries: $\Psi_d \in \mathbb{R}^{N \times N}$, $d = 1, 2, \dots, 8$.

The SNR measurement is adopted to measure the noise level, which is defined as $mSNR = \frac{\|\mathbf{y}\|_2^2}{M\sigma^2}$, where M and σ^2 denote the number of \mathbf{y} and the variance of the white Gaussian noise, respectively. The higher the value of mSNR, the weaker of the noise level is. We evaluate the performance by the popular recovery SNR: $RSNR = -20 \log(\frac{\|\mathbf{x} - \hat{\mathbf{x}}\|_2}{\|\mathbf{x}\|_2})$, where $\hat{\mathbf{x}}$ denotes the estimated sparse image. The higher the value of $RSNR$, the better the performance. We conduct the experiments by utilizing the well-known figure of ‘‘Cameraman’’ with $mSNR = M/N = 40$ dB, which is shown in Figure 2a. To reduce the computation time, we choose only a part of the figure, shown in Figure 2b.

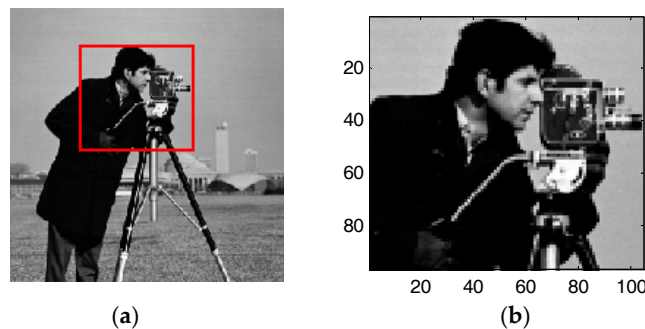


Figure 2. (a) the cropped Cameraman image of size $N = 256 \times 256$. (b) the selected image portion of size $N = 96 \times 104$.

4.1. The Value Range of α in $\lambda_{d,p}$

In Section 4.1, we first determine the value range for α in $\lambda_{d,p}$ by evaluating the performances with different values of α . The results are shown in Figures 3 and 4. From the results, we can find that when $\alpha \in (0, p)$, the proposed algorithms perform well and enjoy strong robustness. With the increase of α , the performances deteriorate rapidly. Therefore, we estimate that the value of α should be $[0, p]$ to obtain the adaptive weighting. We specially set:

$$\lambda_{d,p}^t = \frac{N_d}{(\epsilon + \|\Psi_d \mathbf{x}\|_2^2)^{\frac{1-p}{2}}}, \tag{33}$$

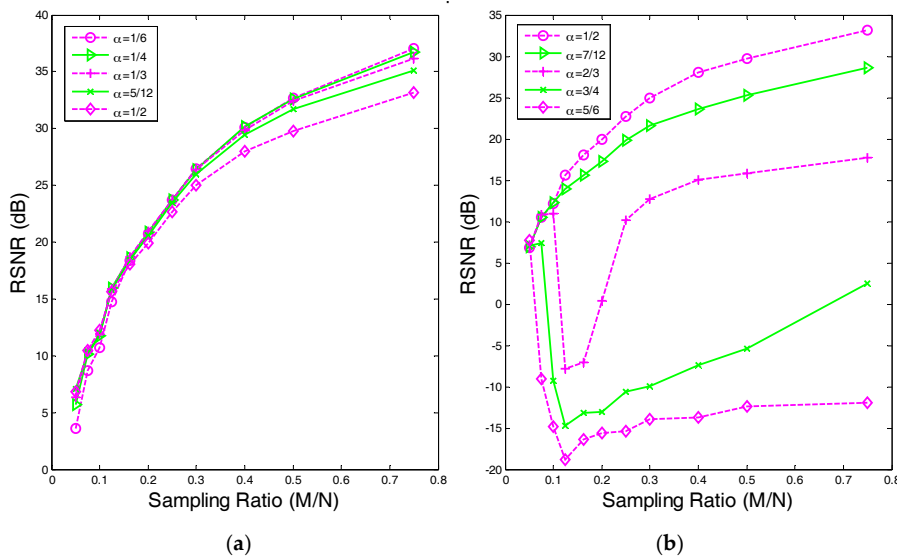


Figure 3. The RSNR of the proposed SAITA- L_p algorithm of $\alpha \in (0, 2p)$ and $p = 1/2$. (a) The RSNR of $\alpha \in \{1/6, 1/4, 1/3, 5/12, 1/2\}$. (b) The RSNR of $\alpha \in \{1/2, 7/12, 2/3, 3/4, 5/6\}$.

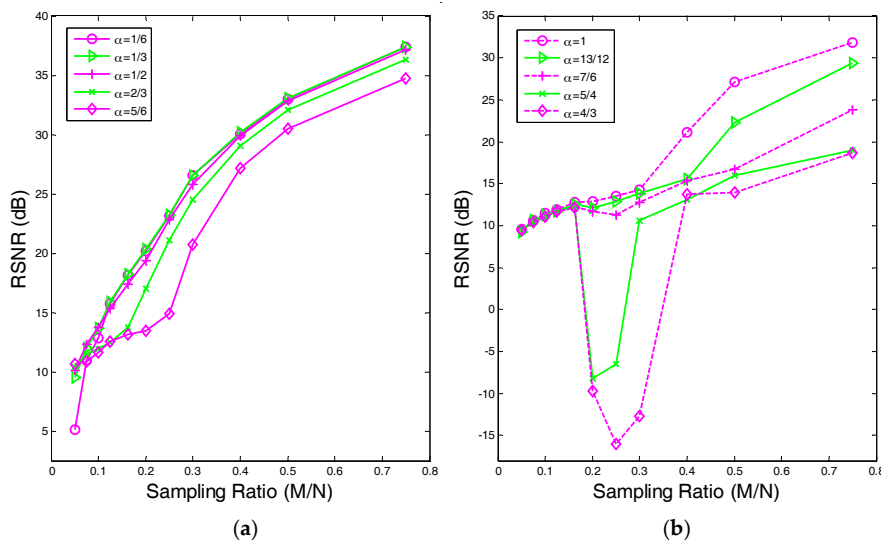


Figure 4. The recovery SNR of the proposed SAITA- L_p algorithm of $\alpha \in (0, 2p)$ and $p = 2/3$. (a) The RSNR versus Sampling Ratio of $\alpha \in \{1/6, 1/3, 1/2, 2/3, 5/6\}$; (b) The RSNR versus Sampling Ratio of $\alpha \in \{1, 13/12, 7/6, 5/4, 4/3\}$.

4.2. The Recovery SNR Performances Versus Sampling Ratio

In Section 4.2, we evaluate the robustness of the proposed algorithm by considering the RSNR versus the sampling ratio. Specifically, we set three mSNR levels to 25 dB, 30 dB and 35 dB. Figure 5 depicts the RSNR versus the sampling ratio. Based on the results, the proposed SAITA- L_p , ($p \in \{1/2, 2/3\}$) algorithm performs better than the conventional single dictionary based algorithm, and the robustness of the proposed algorithm is good.

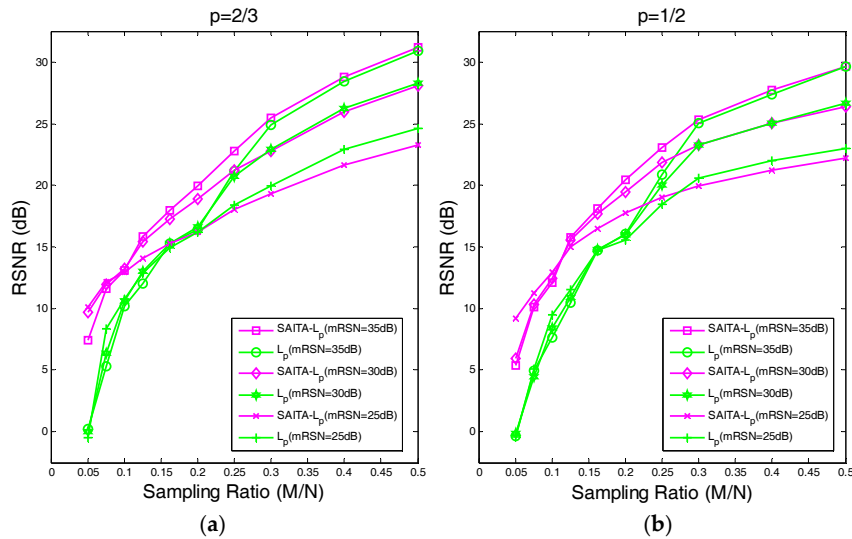


Figure 5. The RSNR performances of the proposed SAITA- L_p algorithm and the L_p algorithm with $mRSN \in \{25, 30, 35\}$ dB. (a) $p = 1/2$. (b) $p = 2/3$.

4.3. The Recovery SNR Performance Versus Measurement SNR

For our third experiment, we investigate the influence of different noise levels on the proposed algorithm and compare the L_p algorithm and Co-L1 [28]. Similarly, we consider three sampling ratio levels of $M/N \in \{0.15, 0.20, 0.25\}$. We evaluate the performance by the RSNR versus the lower mSNR (20 dB~40 dB) of the image, and the results are presented in Figure 6.

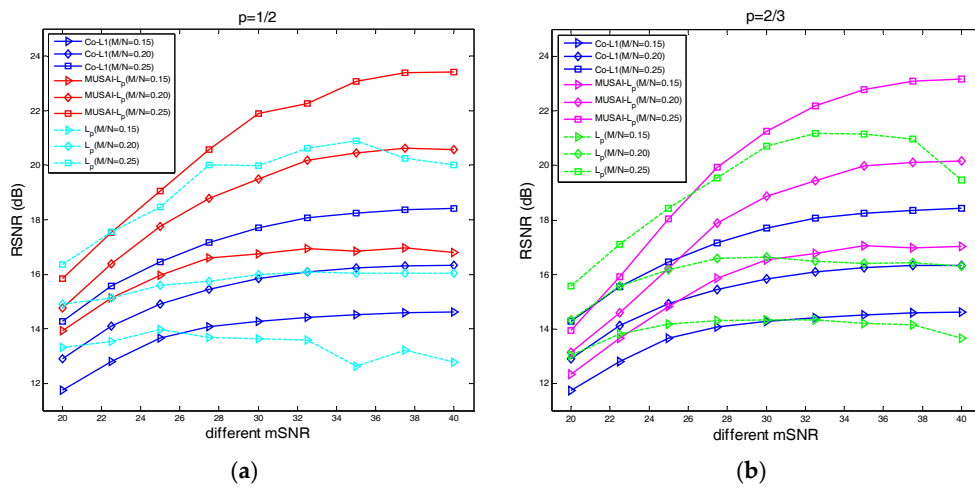


Figure 6. (a) The case of $p = 1/2$ for the sampling ratios $M/N \in \{0.15, 0.20, 0.25\}$ of the Cameraman images. (b) The case of $p = 2/3$ for the sampling ratios $M/N \in \{0.15, 0.20, 0.25\}$ of the cameraman images. The RSNR versus mSNR of the proposed SAITA- L_p ($p \in \{1/2, 2/3\}$) algorithm and the L_p ($p \in \{1/2, 2/3\}$) algorithm for three low sampling ratios $M/N \in \{0.15, 0.20, 0.25\}$.

From the results, we can find that the proposed SAITA- L_p , ($p \in \{1/2, 2/3\}$) algorithm can obtain a higher recovery SNR and has better robustness and fidelity than the Co-L1. The robustness and fidelity of the corresponding L_p , ($p \in \{1/2, 2/3\}$) algorithm will deteriorate with the increase of the signal measurement SNR.

4.4. The Relative Error Performances Versus the Number of Iterations

We study the convergence and the reconstruction error by the relative error performances versus the number of iterations. Choosing the relative error as the second quality measurement, the formula is given:

$$\text{Relative Error} = \frac{\|\mathbf{x} - \hat{\mathbf{x}}\|_2}{\|\mathbf{x}\|_2} \quad (34)$$

Considering the proposed SAITA- L_p , ($p \in \{1/2, 2/3\}$) and the corresponding L_p , ($p \in \{1/2, 2/3\}$) algorithm from the result shown in Figure 7, when the sampling ratio is 0.2 (shown in (a)), the relative errors of the proposed SAITA- L_p , ($p \in \{1/2, 2/3\}$) algorithm are significant smaller, and converge faster than the corresponding L_p , ($p \in \{1/2, 2/3\}$) algorithm. When the sampling ratio is 0.5 (shown in (b)), though the final relative errors are close, the convergence speed of the proposed algorithm is higher (the number of iterations are approximately 15 and 7, respectively). While compared to Co-L1 [28], our proposed SAITA- L_p algorithm can obtain a markedly lower relative error when the sampling ratio is $M/N \in \{0.2, 0.5\}$. In addition, one can observe that the relative error is slightly smaller than for $p = 2/3$, while the convergence rate is faster than the $p = 1/2$.

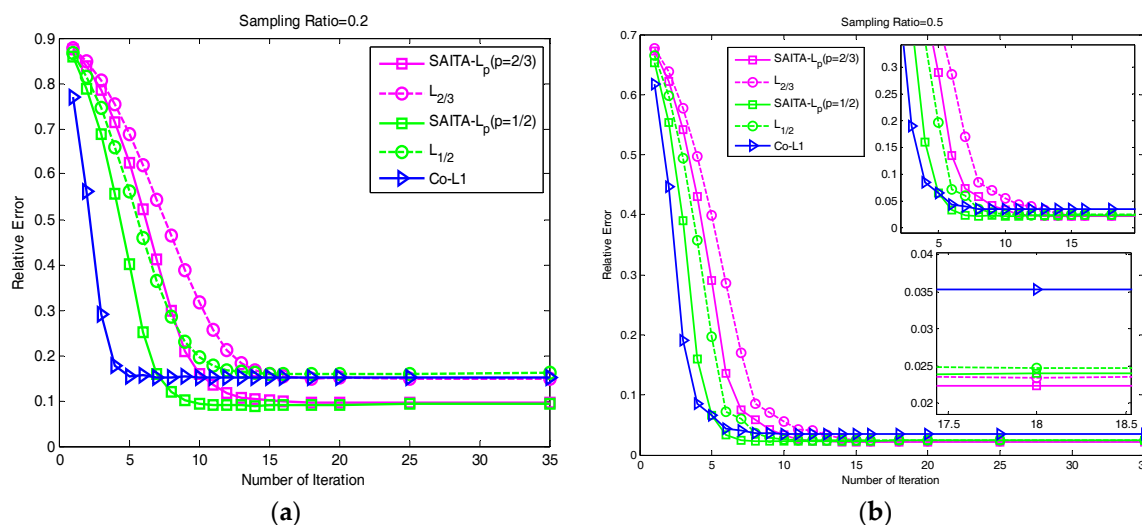


Figure 7. (a) The relative error for the lower sampling ratio $M/N = 0.2$ in the cameraman image. (b) The relative error for the higher sampling ratio of $M/N = 0.5$ in the cameraman image. The relative errors verse the iteration number of the proposed SAITA- L_p algorithm and the L_p algorithm.

5. Practical Experiments

The proposed algorithms can be applied in many practical applications [36–42]. In this section, we conduct some typical applications about sparse image recovery and medical imaging to extend the applications of $L_{1/2}$ and $L_{2/3}$ regularizations and illustrate the excellent robustness and adaptation of the proposed SAITA- L_p , ($p \in \{1/2, 2/3\}$) algorithm. The conventional single dictionary analysis L_p iterative thresholding algorithms [24,25] and the Co-L1 [28] as the standard algorithms for comparison.

5.1. Application 1: Image Sparse Restoration

In the first application, the proposed SAITA- L_p algorithm is applied to restoring the “Cameraman” image shown in Figure 2 versus sampling ratio M/N . We use the reduced $N = 96 \times 104$ cameraman image as the objective image. Figure 8a,c show the recovery results using the conventional single dictionary algorithm of L_1 and L_p , ($p \in \{1/2, 2/3\}$), respectively. Figure 8b,d show the recovery images using the corresponding multiple sub-dictionary algorithm of L_1 and L_p ($p \in \{1/2, 2/3\}$), respectively. The experiments show that all the algorithms can recover the images, and the proposed multiple sub-dictionary algorithms significantly outperform the conventional single-dictionary algorithms. In Figure 9, we depict the RSNR of four algorithms vs. different sampling ratios. When $p = 1/2$ and $p = 2/3$, it can be observed that the proposed SAITA algorithm can obtain a larger RSNR compared with the conventional L_p algorithms. There is no obvious improvement between the two cases of $p = 1/2$ and $p = 2/3$, and the SAITA- $L_{1/2}$ algorithm outperforms the SAITA- $L_{2/3}$ algorithm with a weak advantage.

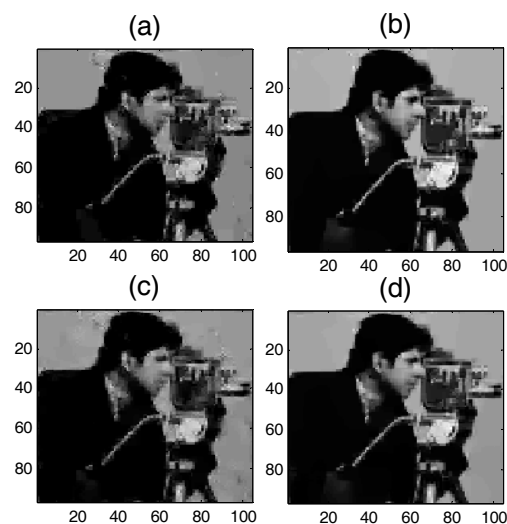


Figure 8. The recovery effects of the proposed SAITA- L_p ($p \in \{1/2, 2/3\}$) and the conventional L_p ($p \in \{1/2, 2/3\}$) algorithms for the $M/N = 0.2$ and $mSNR = 40$ dB cameraman image. (a) $L_{1/2}$, RSNR = 15.7316 dB; (b) SAITA- L_p algorithm ($p = 1/2$), RSNR = 20.5714 dB; (c) $L_{2/3}$, RSNR = 16.3098 dB; and (d) SAITA- L_p algorithm ($p = 2/3$), RSNR = 20.1259 dB.

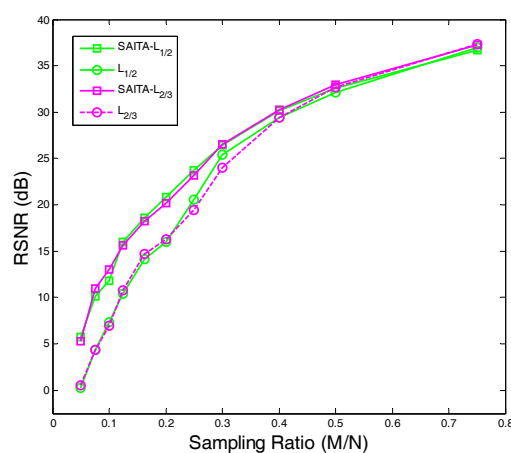


Figure 9. The RSNR of the SAITA- L_p ($p \in \{1/2, 2/3\}$) algorithms vs. the sampling ratio M/N for the $mSNR = 40$ dB cameraman image.

5.2. Application 2: Medical Imaging

In the application 2, we extend the applications of our proposed algorithm to solve typical medical construction problems. We first consider the well-known Shepp-Logan phantom, and then we construct a high-quality dMRI cardiac cine [8,28].

5.2.1. Test 1 for the Shepp-Logan Model

In the test 1, we first consider the well-known Shepp-Logan phantom of $N = 96 \times 96$ with an $mSNR = 40$ dB. We construct the compressed noisy measurement signal \mathbf{y} by utilizing the ‘‘Spread Spectrum’’ operator as the measurement matrix Φ [35], and we conduct a sparsifying transform with the constructed operator $\Psi \in R^{(4N) \times N}$ (‘‘db3’, $N = 1$).

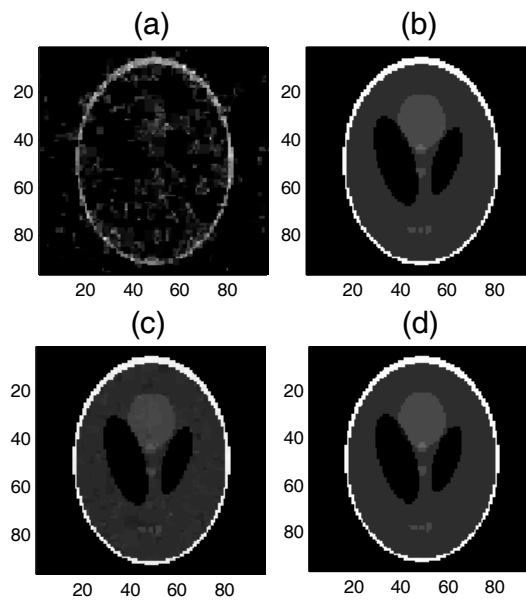


Figure 10. The recovery effects of the proposed $SAITA-L_p$ ($p \in \{1/2, 2/3\}$) and the corresponding L_p ($p \in \{1/2, 2/3\}$) algorithm for the $M/N = 0.140$, $mSNR = 40$ dB Shepp-Logan image. (a) $L_{1/2}$, $RSNR = 3.5436$ dB; (b) $SAITA-L_p$ algorithm ($p = 1/2$), $RSNR = 43.7016$ dB; (c) $L_{2/3}$, $RSNR = 27.2450$ dB; and (d) $SAITA-L_p$ algorithm ($p = 2/3$), $RSNR = 44.9549$ dB.

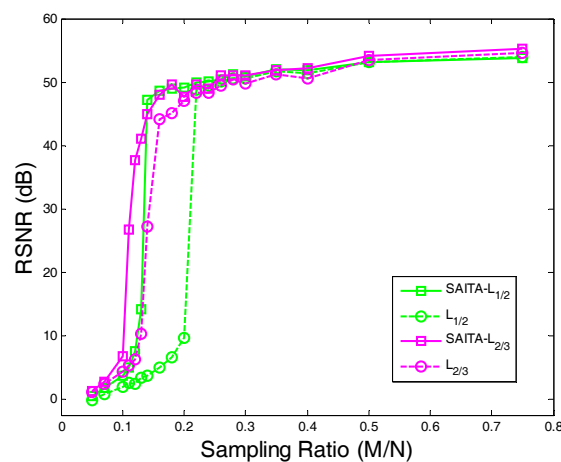


Figure 11. The $RSNR$ of the proposed $SAITA-L_p$ ($p \in \{1/2, 2/3\}$) algorithm and the conventional L_p ($p \in \{1/2, 2/3\}$) algorithm vs. the sampling ratio M/N for the $mSNR = 40$ dB Shepp-Logan image.

From the experimental results shown in Figure 10, we find that the proposed SAITA- L_p algorithm can recover the images perfectly, as shown in Figure 10b,d, while the conventional single dictionary algorithms failed to recover the image, which is shown in Figure 10a,c. The proposed SAITA- L_p algorithm of $p = 2/3$ can obtain the best effect compared with the other algorithms, and the next best is the SAITA- L_p algorithm of $p = 1/2$. In Figure 11, we depict the RSNR of the respective algorithms versus different sampling ratios M/N . When $p = 1/2$ and $p = 2/3$, it can be observed that the proposed SAITA- L_p algorithms can obtain a larger RSNR than the L_p algorithms with $M/N \in (0.1, 0.2)$ significantly.

5.2.2. Test 2 for Real-World Data (2D MRI)

MRI is a typical medical inverse problem that can be solved well by CS [8]. In this experiment, we apply the proposed algorithm to real-world medical data. We investigate a simplified “dynamic MRI” problem [8] and use the high-quality MRI cardiac cine as the ground truth and select a spatio-temporal slice of 144×48 [28]. We construct the sparse matrix $\Psi \in R^{3N \times N}$ with a vertical concatenation of ‘db1’ and ‘db2’ orthogonal discrete wavelet bases with two levels of decomposition (‘db1’, ‘db2’, and $N = 2$). Figure 12 presents the constructed MRI images using the SAITA- L_p ($p \in \{1/2, 2/3\}$) algorithm and L_p ($p \in \{1/2, 2/3\}$) algorithms. From the experiment results, we can see that the proposed SAITA algorithm can reconstruct the images perfectly, as shown in Figure 12b,d, while the conventional algorithms failed to restore the image in Figure 12a,c. The proposed multiple sub-dictionaries algorithm of $p = 2/3$ obtained the best effect and the corresponding recovery SNR is 23.1872 dB. Next is the proposed algorithm of $p = 1/2$ with recovery SNRs of 21.0189 dB. In Figure 13, we depict the RSNR of four algorithms versus different sampling ratios M/N . When $p = 1/2$ and $p = 2/3$, it can be observed that the proposed SAITA- L_p algorithms can obtain a larger RSNR compared with the conventional single dictionary L_p algorithms. The results also show that the algorithms of $p = 2/3$ outperform the methods of $p = 1/2$. That is to say, the $L_{2/3}$ regularization can exploit more prior knowledge than $L_{1/2}$ regularization in MRI.

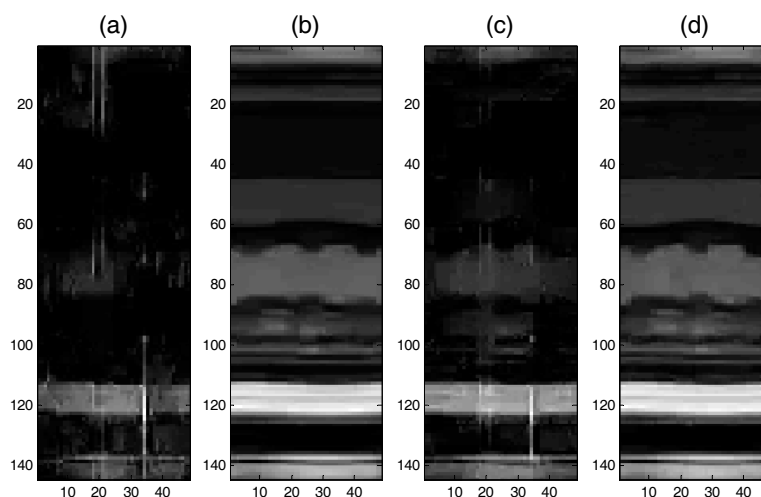


Figure 12. The recovery effects of the proposed SAITA- L_p ($p \in \{1/2, 2/3\}$) and the corresponding $L_{1/2}$ and $L_{2/3}$ algorithm for the $M/N = 0.2$, $mSNR = 40$ dB 2D MRI image. (a) $L_{1/2}$ algorithm, $RSNR = 3.6346$ dB; (b) SAITA- $L_{1/2}$ algorithm, $RSNR = 21.0189$ dB; (c) $L_{2/3}$ algorithm, $RSNR = 7.7718$ dB; and (d) SAITA- $L_{2/3}$ algorithm, $RSNR = 23.1872$ dB.

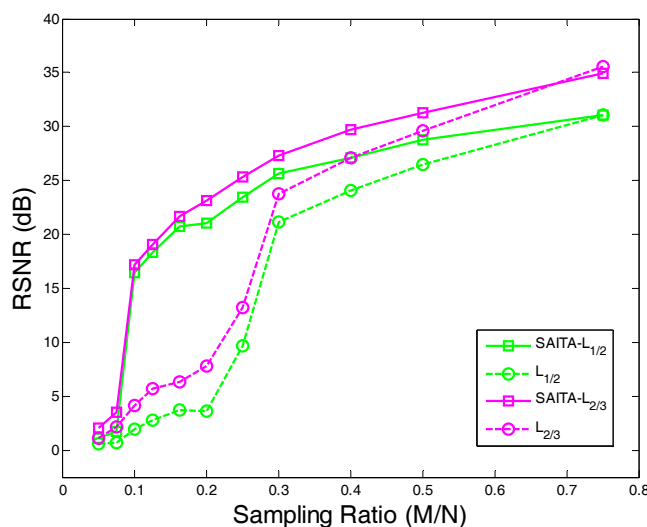


Figure 13. The RSNR of the proposed SAITA- L_p , ($p \in \{1/2, 2/3\}$) algorithm and the L_p , ($p \in \{1/2, 2/3\}$) algorithm versus the sampling ratio for the mSNR = 40 dB 2D MRI image.

6. Conclusions

In this paper, we propose a novel adaptive iteratively weighted thresholding algorithm (SAITA- L_p) based on the conventional $L_{1/2}$ and $L_{2/3}$ thresholding algorithm by incorporating the multiple sub-dictionary sparse representation strategy. We make the following conclusions from the above experiments:

- (1) Using the proposed multiple sub-dictionary sparsifying transforms strategy, we construct a multiple sub-dictionary based L_p regularization method to exploit more priori knowledge of images for the sparse image recovery problem. By multiplying by the proposed adaptive weighting parameter $\lambda_{d,p}^t = \frac{N_d}{(\epsilon + \|\mathbf{\Psi}_d \mathbf{x}\|_2^2)^{\frac{1-p}{2}}}$, we can gain more control of weighting the contribution of each sub-dictionary based regularizer. Experiments show that the proposed algorithms appear to perform better than the conventional single-dictionary algorithms, especially when the sampling rate is very low (e.g., 0.1~0.3);
- (2) Compared with the L_1 -norm regularization based work, the nonconvex L_p ($0 < p < 1$)-norm penalty can more closely approximate the L_0 -norm minimization over the L_1 -norm, which gives a sparser solution and needs fewer measurement data.
- (3) In our experiments, we find that the recovery performances between the L_p ($p = 1/2$) and L_p ($p = 2/3$) are close, even when the corresponding $p = 2/3$ algorithm can obtain a better performance over the $p = 1/2$. Hence, a proper p need to be selected in practical applications.
- (4) Moreover, the proposed SAITA- L_p method also indicates that it is feasible to improve the recovery performance by exploiting the signal inner sparse structure and designing a proper sparse representation dictionary. Thus, it is beneficial to exploit the signal sparse structure with a dictionary learning method, which will be the subject of future work.
- (5) The proposed SAITA- L_p algorithm can be extended to other non-convex penalties include smoothly clipped absolute deviation (SCAD) and minimax concave penalty (MCP).

Acknowledgments: This work was supported by National Natural Science Foundation of China grants (No. 61401069, No. 61701258); Jiangsu Specially Appointed Professor Grant (RK002STP16001); Innovation and Entrepreneurship of Jiangsu High-level Talent Grant (CZ0010617002), High-level talent startup grant of Nanjing University of Posts and Telecommunications (XK0010915026), Natural Science Foundation of Jiangsu Province Grant (No. BK20170906), Natural Science Foundation of Jiangsu Higher Education Institutions Grant (No. 17KJB510044) “1311 Talent Plan” of Nanjing University of Posts and Telecommunications as well as Postgraduate Research Innovation Program, Jiangsu (KYLX16_0647).

Author Contributions: Yunyi Li, Jie Zhang, Jian Xiong proposed the SAITA algorithm. Jie Yang and Jian Xiong conceived and designed the experiments; Shanggang Fan performed the practical experiments; Yunyi Li and Guan Gui analyzed the data; Yunyi Li, Guan Gui and Jie Yang wrote the paper. Xiefeng Cheng, Hikmet Sari and Fumiyuki Adachi checked this paper.

Conflicts of Interest: The authors declare no conflict of interest.

References

1. Donoho, D.L. Compressed sensing. *IEEE Trans. Inf. Theory* **2006**, *52*, 1289–1306. [[CrossRef](#)]
2. Candès, E.J.; Romberg, J.; Tao, T. Robust Uncertainty Principles: Exact Signal Frequency Information. *IEEE Trans. Inf. Theory* **2006**, *52*, 489–509. [[CrossRef](#)]
3. Wright, J.; Yang, A.Y.; Ganesh, A.; Sastry, S.S.; Ma, Y. Robust face recognition via sparse representation. *IEEE Trans. Pattern Anal. Mach. Intell.* **2009**, *31*, 210–227. [[CrossRef](#)] [[PubMed](#)]
4. Mairal, J.; Elad, M.; Sapiro, G. Sparse representation for color image restoration. *IEEE Trans. Image Process.* **2008**, *17*, 53–69. [[CrossRef](#)] [[PubMed](#)]
5. Gao, Z.; Dai, L.; Qi, C.; Yuen, C.; Wang, Z. Near-Optimal Signal Detector Based on Structured Compressive Sensing for Massive SM-MIMO. *IEEE Trans. Veh. Technol.* **2016**, *9545*, 1–5. [[CrossRef](#)]
6. Gao, Z.; Dai, L.; Wang, Z.; Member, S.; Chen, S.; Hanzo, L. Compressive Sensing Based Multi-User Detector for the Large-Scale SM-MIMO Uplink. *IEEE Trans. Veh. Technol.* **2015**, *9545*, 1–14.
7. Gui, G.; Xu, L.; Adachi, F. Variable step-size based sparse adaptive filtering algorithm for estimating channels in broadband wireless communication systems. *EURASIP J. Wirel. Commun. Netw.* **2014**, *2014*, 1–10. [[CrossRef](#)]
8. Herman, M.; Strohmer, T. Compressed sensing radar. In Proceedings of the 2008 IEEE International Conference on Acoustics, Speech and Signal Processing (ICASSP), Las Vegas, NV, USA, 30 March–4 April 2008; pp. 1509–1512.
9. Chen, G.; Gui, G.; Li, S. Recent results in compressive sensing based image inpainting algorithms and open problems. In Proceedings of the 2015 8th International Congress on Image and Signal Processing, Liaoning, China, 14–16 October 2015.
10. Oh, P.; Lee, S.; Kang, M.G. Colorization-based RGB-white color interpolation using color filter array with randomly sampled pattern. *Sensors* **2017**, *17*, 1523. [[CrossRef](#)] [[PubMed](#)]
11. Candès, E.J. The restricted isometry property and its implications for compressed sensing. *C. R. Math.* **2008**, *346*, 589–592. [[CrossRef](#)]
12. Afonso, M.V.; Bioucas-Dias, J.M.; Figueiredo, M.A.T. Fast image recovery using variable splitting and constrained optimization. *IEEE Trans. Image Process.* **2010**, *19*, 2345–2356. [[CrossRef](#)] [[PubMed](#)]
13. Yang, J.; Zhang, Y. Alternating Direction Algorithms for L1 Problems in Compressive Sensing. *SIAM J. Sci. Comput.* **2009**, *33*, 250–278. [[CrossRef](#)]
14. Beck, A.; Teboulle, M. A Fast Iterative Shrinkage-Thresholding Algorithm for Linear Inverse Problems. *SIAM J. Imaging Sci.* **2009**, *2*, 183–202. [[CrossRef](#)]
15. Becker, S.; Bobin, J.; Candès, E. NESTA: A Fast and Accurate First-order Method for Sparse Recovery. *SIAM J. Imaging Sci.* **2009**, *4*, 1–39. [[CrossRef](#)]
16. Borgerding, M.; Schniter, P.; Vila, J. Generalized Approximate Message Passing for Cosparsity Analysis compressive sensing. In Proceedings of the 2015 IEEE International Conference on Acoustics, Speech and Signal Processing (ICASSP), South Brisbane, Australia, 19–24 April 2015; pp. 3756–3760.
17. Chartrand, R. Exact reconstruction of sparse signals via nonconvex minimization. *IEEE Signal Process. Lett.* **2007**, *14*, 707–710. [[CrossRef](#)]
18. Fan, J.; Li, R. Variable Selection via Nonconcave Penalized Likelihood and its Oracle Properties. *J. Am. Stat. Assoc.* **2001**, *96*, 1348–1360. [[CrossRef](#)]
19. Zhang, C.H. Nearly unbiased variable selection under minimax concave penalty. *Ann. Stat.* **2010**, *38*, 894–942. [[CrossRef](#)]
20. Chartrand, R.; Yin, W. Iteratively reweighted algorithms for compressive sensing. In Proceedings of the 2008 IEEE International Conference on Acoustics, Speech and Signal Processing (ICASSP), Las Vegas, NV, USA, 1 March–4 April 2008; pp. 3869–3872.

21. Blumensath, T.; Davies, M.E. Iterative hard thresholding for compressed sensing. *Appl. Comput. Harmon. Anal.* **2009**, *27*, 265–274. [[CrossRef](#)]
22. Fornasier, M.; Rauhut, H. Iterative thresholding algorithms. *Appl. Comput. Harmon. Anal.* **2008**, *25*, 187–208. [[CrossRef](#)]
23. Marjanovic, G.; Solo, V. On Lq Optimization and Matrix Completion. *IEEE Trans. Signal Process.* **2012**, *60*, 5714–5724. [[CrossRef](#)]
24. Xu, Z.; Chang, X.; Xu, F.; Zhang, H. L 1/2 Regularization: A Thresholding Representation Theory and a Fast Solver. *IEEE Trans. Neural Netw. Learn. Syst.* **2012**, *23*, 1013–1027. [[CrossRef](#)] [[PubMed](#)]
25. Cao, W.; Sun, J.; Xu, Z. Fast image deconvolution using closed-form thresholding formulas of L q ($q = 1/2, 2/3$) regularization. *J. Vis. Commun. Image Represent.* **2013**, *24*, 31–41. [[CrossRef](#)]
26. Ma, J.; März, M.; Funk, S.; Schulz-Menger, J.; Kutyniok, G.; Schaeffter, T.; Kolbitsch, C. Shearlet-based compressed sensing for fast 3D cardiac MR imaging using iterative reweighting. *arXiv* **2017**, arXiv:1705.00463.
27. Ma, J.; März, M. A multilevel based reweighting algorithm with joint regularizers for sparse recovery. *arXiv* **2016**, arXiv:1604.06941.
28. Ahmad, R.; Schniter, P. Iteratively Reweighted L1 Approaches to Sparse Composite Regularization. *IEEE Trans. Comput. Imaging* **2015**, *1*, 220–235. [[CrossRef](#)]
29. Tan, Z.; Eldar, Y.C.; Beck, A.; Nehorai, A. Smoothing and decomposition for analysis sparse recovery. *IEEE Trans. Signal Process.* **2014**, *62*, 1762–1774.
30. Zhang, Y.; Ye, W. L2/3 regularization: Convergence of iterative thresholding algorithm. *J. Vis. Commun. Image Represent.* **2015**, *33*, 350–357. [[CrossRef](#)]
31. Lim, W.Q. The discrete shearlet transform: A new directional transform and compactly supported shearlet frames. *IEEE Trans. Image Process.* **2010**, *19*, 1166–1180. [[PubMed](#)]
32. Zhang, W.; Gao, F.; Yin, Q. Blind Channel Estimation for MIMO-OFDM Systems with Low Order Signal Constellation. *IEEE Commun. Lett.* **2015**, *19*, 499–502. [[CrossRef](#)]
33. Daubechies, I. *Ten Lectures on Wavelets*; Society for Industrial and Applied Mathematics: Philadelphia, PA, USA, 1992.
34. Zeng, J.; Lin, S.; Wang, Y.; Xu, Z. L1/2 regularization: Convergence of iterative half thresholding algorithm. *IEEE Trans. Signal Process.* **2014**, *62*, 2317–2329. [[CrossRef](#)]
35. Puy, G.; Vandergheynst, P.; Gribonval, R.; Wiaux, Y. Universal and efficient compressed sensing by spread spectrum and application to realistic Fourier imaging techniques. *EURASIP J. Adv. Signal Process.* **2012**, 2012. [[CrossRef](#)]
36. Liu, A.; Zhang, Q.; Li, Z.; Choi, Y.J.; Li, J.; Komuro, N. A green and reliable communication modeling for industrial internet of things. *Comput. Electr. Eng.* **2017**, *58*, 364–381. [[CrossRef](#)]
37. Li, H.; Dong, M.; Ota, K.; Guo, M. Pricing and Repurchasing for Big Data Processing in Multi-Clouds. *IEEE Trans. Emerg. Top. Comput.* **2016**, *4*, 266–277. [[CrossRef](#)]
38. Chen, Z.; Liu, A.; Li, Z.; Choi, Y.J.; Sekiya, H.; Li, J. Energy-efficient broadcasting scheme for smart industrial wireless sensor networks. *Mob. Inform. Syst.* **2017**. [[CrossRef](#)]
39. Wu, J.; Ota, K.; Dong, M.; Li, J.; Wang, H. Big data analysis based security situational awareness for smart grid. *IEEE Trans. Big Data* **2016**, *99*, 1–11. [[CrossRef](#)]
40. Hu, Y.; Dong, M.; Ota, K.; Liu, A.; Guo, M. Mobile target detection in wireless sensor networks with adjustable sensing frequency. *IEEE Syst. J.* **2016**, *10*, 1160–1171. [[CrossRef](#)]
41. Chen, Z.; Liu, A.; Li, Z.; Choi, Y.J.; Li, J. Distributed Duty cycle control for delay improvement in wireless sensor networks. *Peer-to-Peer Netw. Appl.* **2017**, *10*, 559–578. [[CrossRef](#)]
42. Kato, N.; Fadlullah, Z.M.; Mao, B.; Tang, F.; Akashi, O.; Inoue, T.; Mizutani, K. The Deep Learning Vision for Heterogeneous Network Traffic Control: Proposal, Challenges, and Future Perspective. *IEEE Wirel. Commun.* **2017**, *24*, 146–153. [[CrossRef](#)]

